

EFFECT OF SINUSOIDAL WAVY WALL ON HEAT TRANSFER FROM DISCRETE HEAT SOURCES PLACED IN TWO- DIMENSIONAL CHANNEL

Dr. Ahmed W. Musatfa
Mech.Engr.Dept.
College of Engineering
University of Tikrit

Dr. Hameed J. Khalif
Mech.Eng.Dept.
College of Engineering
University of Tikrit

Hasan H. Ali
Mech.Eng.Dept.
College of Engineering
University of Tikrit

ABSTRACT

The effect of wavy wall in a two dimensional channel on heat transfer from three isothermal heat sources placed on the lower wall of the channel has been investigated numerically. Four cases have been considered in this study, in each case the wavy wall is on the upper wall of the channel while the heat sources are placed on the lower wall of the channel. The flow and temperature field are studied numerically with different amplitude to channel height ratios and different number of waves. The laminar flow field is analyzed numerically by solving the steady forms of the two-dimensional incompressible Navier- Stokes and energy equations. The Cartesian velocity components and pressure on a collocated (non-staggered) grid are used as dependent variables in the momentum equations, which is discretized by finite volume method, body fitted coordinates are used to represent the complex wavy wall accurately, and grid generation technique based on elliptic partial differential equations is employed. SIMPLE algorithm is used to adjust the velocity field to satisfy the conservation of mass. The range of Reynolds number is ($50 \leq Re \leq 1000$) and the range of the wave amplitude is ($-0.5 \leq A \leq 0.5$) and the Prandtl number is (0.7).

The results show that the maximum heat transfer enhancement in the studied cases is in the case where the wavy wall placed on the upper wall over the sources and half wave over each source.

KEYWORDS: Wavy Wall, Finite Volume, Discrete Heat Sources, Channel

تأثير الجدار المتموج جيبا على انتقال الحرارة من مصادر حرارية متقطعة في قناه ثنائية البعد

م.م. حسن حمد علي
كلية الهندسة - جامعة تكريت

د.حميد جاسم خلف
كلية الهندسة - جامعة تكريت

د.احمد وحيد مصطفى
كلية الهندسة - جامعة تكريت

الخلاصة

تم إجراء دراسة عددية لتأثير جدار متموج لقناة ثنائية البعد على الحرارة المنتقلة من ثلاثة مصادر حرارية ذات درجة حرارة ثابتة موضوعة على الجدار السفلي للقناة حيث تم دراسة اربع حالات، في جميع الحالات الجدار المتموج هو الجدار العلوي للقناة بينما وضعت المصادر الحرارية على الجدار السفلي للقناة. تم دراسة حقلتي الجريان ودرجة الحرارة عدديا لقيم مختلفة لنسبة سعة الموجة إلى ارتفاع القناة ولعدد موجات مختلف أيضا. تم تحليل حقلتي الجريان عدديا بحل معادلات نافير- ستوكس والطاقة الثنائية الأبعاد واللانضغاطية للحالة المستقرة. تم استخدام مركبات السرعة الديكارتية والضغط على شبكة متحدة الموقع كمتغيرات معتمدة في معادلة الزخم التي تم تقطيعها بطريقة الحجم المحدد، ومن اجل تمثيل شكل القناة المعقد بشكل دقيق تم استخدام إحداثيات مطابقة الجسم، وتم استخدام طريقة توليد الشبكة على أساس معادلات تفاضلية جزئية بيضوية. استخدمت خوارزمية SIMPLE لتعديل حقل السرعة لكي تحقق حفظ الكتلة. تم اخذ رقم رينولدز ضمن المدى ($50 \leq Re \leq 1000$) وسعة الموجة بين ($-0.5 \leq A \leq 0.5$) ورقم براندتل (0.7). بينت النتائج أن الحالة الأمثل بين الحالات المدروسة لتحسين عملية انتقال الحرارة هي حالة وضع التموج على الجدار العلوي فوق مصادر الحرارة بحيث تكون نصف موجة فوق كل مصدر.

NOMENCLATURE

b	Distance before the sources on the upper wall
G_1	Contravariant velocity in ζ direction
G_2	Contravariant velocity in η direction
H	Dimensionless channel height
J	Jacobian transformation
L	Channel length (m)
w	Number of waves
Nu	Average Nusselt number
Nu_L	Average Nusselt number based on channel length
p	Pressure (Pa)
P	Dimensionless pressure
Pr	Prandtl number
Re	Reynolds number
s	Distance before the sources on the upper wall
S_ϕ	Source term
U	Dimensionless velocity in X-direction
U_m	Dimensionless mean velocity
V	Dimensionless velocity in Y-direction
X	Dimensionless axial coordinate
Y	Dimensionless vertical coordinate
α, β, γ	Dimensionless coordinate transformation parameters
Γ	Dimensionless diffusion coefficient
λ	Wave length (m)
μ	Viscosity (Pa.s)
ζ, η	Dimensionless curvilinear coordinates
ρ	Density (Kg/m ³)
ϕ	Dimensionless dependent variable

INTRODUCTION

The use of enhanced surfaces allows the designer to increase the heat duty for a given exchanger, usually with pressure drop penalty, or to reduce the size of heat exchanger for a given heat duty. The wavy channel is typically employed in compact heat exchangers for enhancing heat transfer. The geometrical complexity of this channel significantly affects the flow pattern and also the heat transfer. [Goldstein and Sparrow 1977] were the first to use the naphthalene technique to measure local and average heat transfer coefficients in a corrugated wall channel (with 'triangular waves'). Their experiments in laminar, transitional and turbulent flows used two corrugation cycles (i.e. two wavelengths). They observed secondary flows in the regions of high resolution local and average mass transfer measurement, and comparison of their results with those obtained with parallel plate channels showed a threefold enhancement in the average heat transfer in the turbulent régimes. However, there was an even greater penalty in the pumping power required.

[Wang and Chen 2002] have analyzed the rates of heat transfer for flow through a sinusoidally curved converging-diverging channel using a simple coordinate transformation and spline alternating-direction implicit method under the assumption of Newtonian and incompressible fluid and laminar, incompressible and two dimensional flow. They studied the effects of the wavy geometry, Reynolds number and Prandtl number on the skin friction and Nusselt number. They showed that the amplitudes of the Nusselt number and the skin friction coefficient increase with an increase in the Reynolds number and amplitude-wavelength ratio. The heat transfer enhancement is not significant at smaller amplitude-wavelength ratio; however, at a sufficiently larger value of amplitude-wavelength ratio the corrugated channel will be an effective heat transfer device, especially at higher Reynolds numbers. [Haitham etc 2005] studied a two-dimensional steady developing fluid flow and heat transfer through a periodic wavy passage numerically for a fluid with a Prandtl number of 0.7 and compared to flow through a corresponding straight (parallel-plate) channel. Sinusoidal and arc-shaped configurations were studied for a range of geometric parameters. They found that at low Reynolds number, the two geometric configurations showed little or no heat transfer augmentation in comparison with a parallel-plate channel. In some cases the heat transfer enhancement ratios were as high as 80% at higher Reynolds number. An increase in either the height ratio or the length ratio for both sine and arc-shaped configurations resulted in a decrease in the recirculation size and strength.

Periodically fully developed flow was attained downstream of the first module of the six modules considered in this study.

[Esam and Raed 2009] studied Periodic vortex shedding in pulsating flow inside wavy channel and the effect it has on heat transfer using the finite volume method. A sinusoidal-varying component is superimposed on a uniform flow inside a sinusoidal wavy channel and the effects on the Nusselt number are analyzed. They found that a unique optimum value of the pulsation frequency, represented by the Strouhal number, exists for Reynolds numbers ranging from 125 to 1000. Results suggest that the gain in heat transfer is related to the process of vortex formation, movement about the troughs of the wavy channel, and subsequent ejection/destruction through the converging section. Heat transfer is the highest when the frequencies of the pulsation and vortex formation approach being in-phase. Analysis of Strouhal number effect on Nu over a period of pulsation substantiates the proposed physical mechanism for enhancement. The effect of changing the amplitude of pulsation is also presented over a period of pulsation, showing a monotonic increase in heat transfer with increasing amplitude. The 60% increase in Nusselt number suggests that sinusoidal fluid pulsation can an effective method for enhancing heat transfer in laminar, wavy-channel flows.

In this work, numerical study has been conducted to investigate the effect of the wavy geometry on the heat transfer from discrete heat sources distributed on the lower wall of the wavy taking into account other effective parameters that have not been covered by previous researchers such as the discrete heating.

MATHEMATICAL MODEL

The laminar flow considered is that of constant-properties, fully-developed, incompressible, Newtonian fluid in a two-dimensional channel with upper wavy wall. The flow is governed by the Navier-Stokes and energy equations. Based on the characteristic scales of channel height (H), average inlet velocity U_m , temperature difference between the sources wall temperature and the inlet temperature ($T_w - T_o$), the dimensionless variables are defined as follows:

$$(X, Y) = \frac{(x, y)}{H}, \quad (U, V) = \frac{(u, v)}{U_m}, \quad P = \frac{p}{\rho U_m^2}, \quad \theta = \frac{T - T_o}{T_w - T_o}$$

The two basic dimensionless groups describing the problem are the Reynolds Re and Prandtl Pr numbers, and they are defined as, respectively

$$\text{Re} = \frac{\rho U_m H}{\mu}, \quad \text{Pr} = \frac{\mu C_p}{k}$$

Considering the above dimensionless variables and groups, the dimensionless governing equations are as follows:

$$\frac{\partial U}{\partial X} + \frac{\partial V}{\partial Y} = 0 \quad (1)$$

$$\frac{\partial U^2}{\partial X} + \frac{\partial UV}{\partial Y} = -\frac{\partial P}{\partial X} + \frac{1}{\text{Re}} \left(\frac{\partial^2 U}{\partial X^2} + \frac{\partial^2 U}{\partial Y^2} \right) \quad (2)$$

$$\frac{\partial UV}{\partial X} + \frac{\partial V^2}{\partial Y} = -\frac{\partial P}{\partial Y} + \frac{1}{\text{Re}} \left(\frac{\partial^2 V}{\partial X^2} + \frac{\partial^2 V}{\partial Y^2} \right) \quad (3)$$

$$\frac{\partial U\theta}{\partial X} + \frac{\partial V\theta}{\partial Y} = \frac{1}{\text{Re Pr}} \left(\frac{\partial^2 \theta}{\partial X^2} + \frac{\partial^2 \theta}{\partial Y^2} \right) \quad (4)$$

Boundary conditions in the physical flow domain are shown in **Fig. 2**. At the inlet of the channel, parabolic velocity distribution has been considered. Pressure, is assumed to be unchanging in the flow direction at the inlet, therefore, the inlet should be located far enough upstream of the heat sources to ensure that this assumption is valid and specified temperature is assumed. At the exit plane the values of the dependent variables are unknown, except the temperature which has

specified value. Therefore, the outlet boundary should be placed far down from the region of interest, at a location where the flow properties are not varied. The outlet properties can be found by set the stream wise derivatives (gradients) of all unknown variables to zero. All the velocity components are set to zero on all solid boundaries (channel surfaces). Wall pressure and temperature are determined by setting the pressure and temperature gradient normal to the surface equal to zero except the source surface temperature which has constant known value.

WAVE MODEL

The wave used in the present study is sinusoidal wave which has variable wave amplitude and number of waves. It is inserted in the mathematical model according to the following equations:

$$Y = A \sin(2\pi w(((x/H) - (b/H))/(w(\lambda/H)))) + 1 \quad (5)$$

Where A is the dimensionless wave amplitude, λ is the wave length, and w is the number of waves

NUMERICAL SOLUTION

The set of conservation equations (1-4) can be written in general form in Cartesian coordinates as

$$\frac{\partial(U\phi)}{\partial X} + \frac{\partial(V\phi)}{\partial Y} = \frac{\partial}{\partial X} \left(\Gamma \frac{\partial \phi}{\partial X} \right) + \frac{\partial}{\partial Y} \left(\Gamma \frac{\partial \phi}{\partial Y} \right) + S_\phi \quad (6)$$

Where Γ is the effective diffusion coefficient, ϕ is the general dependent variable, S_ϕ is the source term.

The grid generation scheme based on elliptic partial differential equations is used in the present study to generate the curvilinear coordinates. In this method, the curvilinear coordinates are generated by solving the following elliptic equations

$$\left. \begin{aligned} \alpha \frac{\partial^2 X}{\partial \zeta^2} - 2\gamma \frac{\partial^2 X}{\partial \zeta \partial \eta} + \beta \frac{\partial^2 X}{\partial \eta^2} &= 0 \\ \alpha \frac{\partial^2 Y}{\partial \zeta^2} - 2\gamma \frac{\partial^2 Y}{\partial \zeta \partial \eta} + \beta \frac{\partial^2 Y}{\partial \eta^2} &= 0 \end{aligned} \right\} \quad (7)$$

Where α, β, γ are the coefficients of transformation. They are expressed as

$$\alpha = \left(\frac{\partial X}{\partial \eta} \right)^2 + \left(\frac{\partial Y}{\partial \eta} \right)^2, \quad \gamma = \left(\frac{\partial X}{\partial \zeta} \frac{\partial X}{\partial \eta} \right) + \left(\frac{\partial Y}{\partial \zeta} \frac{\partial Y}{\partial \eta} \right), \quad \beta = \left(\frac{\partial X}{\partial \zeta} \right)^2 + \left(\frac{\partial Y}{\partial \zeta} \right)^2 \quad (8)$$

The grid generation for the wavy channel for number of control volume (81X41) is illustrated in **Figure 6**.

Equation (6) can be transformed from physical domain to computational domain according to the following transformation $\zeta = \zeta(x, y), \eta = \eta(x, y)$, the final form of the transformed equation can be written as:-

$$\frac{\partial}{\partial \zeta} (\phi G_1) + \frac{\partial}{\partial \eta} (\phi G_2) = \frac{\partial}{\partial \zeta} \left(\frac{\Gamma}{J} \left(\alpha \frac{\partial \phi}{\partial \zeta} - \gamma \frac{\partial \phi}{\partial \eta} \right) \right) + \frac{\partial}{\partial \eta} \left(\frac{\Gamma}{J} \left(\beta \frac{\partial \phi}{\partial \eta} - \gamma \frac{\partial \phi}{\partial \zeta} \right) \right) + JS_\phi \quad (9)$$

Where G_1 and G_2 are the contravariant velocity components, J is the Jacobian of the transformation, on the computational plane, and α, β, γ are the coefficients of transformation. They are expressed as

$$G_1 = U \frac{\partial Y}{\partial \eta} - V \frac{\partial X}{\partial \eta}, \quad G_2 = V \frac{\partial X}{\partial \zeta} - U \frac{\partial Y}{\partial \zeta}, \quad J = \left(\frac{\partial X}{\partial \zeta} \frac{\partial Y}{\partial \eta} - \frac{\partial Y}{\partial \zeta} \frac{\partial X}{\partial \eta} \right) \quad (10)$$

The transferred equation (9) is integrated over the control volume in the computation domain. The convective terms are discretized by using hybrid scheme, while the diffusion terms are discretized by central scheme. SIMPLE algorithm on a collocated non-orthogonal grid is used to adjust the velocity field to satisfy the conservation of mass. Since all variables are stored in the center of the control volume, the interpolation method is used in the pressure correction equation to avoid the decoupling between velocity and pressure as in [Rhie and Chow 1983]. In order to consider the effect of the cross derivatives and to avoid solving a nine diagonal matrix of the pressure-correction equation, the cross derivatives are calculated by the approximate method of [Wang and Komori2000]. The resulting set of discretization equations are solved iteratively using the line-by-line procedure which uses the Tri-Diagonal Matrix Algorithm (TDMA). The convergence criterion is that the maximum residuals in all equations fall below 10^{-4} . For further information, numerical details can be found in [Ferziger and Peric 1996].

MODEL VALIDATION

The algorithm is validated against a case of steady flow in a wavy channel. Specifically, the results of [Wang and Chen 2002] are used. That study was for a channel of similar sinusoidally-wavy channel that has six periods, an amplitude-wave length ratio of 0.1, and a fluid Prandtl number of 6.93. A few modifications were made to the current geometry to ensure compatibility. A comparison of the local Nusselt number for the wavy section for wave amplitude ($A=0.1$) is shown in Figure 4. As can be seen, the agreement is very good.

GRID INDEPENDENCY TEST (GIT)

A series of test cases were run to ensure mesh-independent solution. The mesh was gradually refined, until the averaged Nusselt number changed by less than 0.1%. Fig 5 shows that an accuracy test of grid fineness is made for grids of $M \times N$ equal 101×41 , 201×81 and 301×121 for the first source for ($A = 0$) and ($Re = 50$). Comparing the grids of 101×41 and 201×81 it will be observed that there are discrepancies in the Nusselt numbers, this indicates that more grids are required to resolve the temperature field, in order to gain a better result for the Nusselt number. As will be observed more clearly in Fig 5, the results for grids of 201×81 in this study are in good agreement with those obtained by grids of 301×121 . Thus, a 201×81 is used in this study to minimize CPU time.

RESULTS AND DISCUSSION

Four cases have been studied in the present work. As shown in Figure 3 the four cases differs from each other by the number of wave ($w = 1, 3, 6$ and 9). In each case the wave amplitude has been changed from -0.5 to 0.5 and the Reynolds number has been changed from 50 to 1000 . Figure 7(a) shows the effect of wave amplitude on the average Nusselt number for case (1) where the Number of waves $w = 1$ and for $Re = 50$. It is observed that for the first and second sources the variation of the wave amplitude from $A = 0$ to $A = -0.5$ increases the average Nusselt number because of the decreasing in the cross-sectional area which leads to increasing in the velocity (see Figure 8(b)) and as a result the temperature gradient will increase as shown in Figure 9. And the variation of the wave amplitude from $A=0$ to $A=0.5$ did not affect the Nusselt number due to the separation which cancelled the increasing of the area as shown in Figure 9(a). An opposite behavior can be seen for the third source due to its position which makes its conditions opposite to those of the first source.

For case (2) Where the Number of waves $w = 3$ where there is a half wave over each source the average Nusselt number for the three sources as shown in Figure 7(b), the variation in the wave amplitude from $A=0$ to $A=-0.5$ leads to an increase in the Nusselt number because the increasing in the temperature gradient on the wall (Figures 11) resulted from the increasing of the velocity (Figure 10(b)) because the cross-sectional area decreasing as the wave amplitude varies from $A=0$ to $A=-0.5$. The average Nusselt number for the second and third sources is shown in Figure 7(b), it is observed that the average Nusselt number increase with the variation of the wave amplitude from $A=0$ to $A=-0.5$ and from $A=0$ to $A=0.5$, this is due to the increasing in the velocity as shown in Figure 10 (a and b).

Figures 7(c) and (d) show the average Nusselt number respectively for the three heat sources for case (3) where the Number of waves $w = 6$ and case (4) Where the Number of waves $w = 9$. It can be observed that the average Nusselt number increase with the variation of the wave amplitude from $A=0$ to $A=-0.5$ and from $A=0$ to $A=0.5$, this is due to the increasing in the velocity which did not affect by the flow separation, so that

if the number of waves increases to more than one wave over each source the heat transfer is always increasing with respect to flat plate case ($A=0$) and is independent on the value of amplitude.

For the case (1-4) the wavy wall enhance the heat transfer for all the sources and the maximum heat transfer enhancement and the corresponding wave amplitude values are presented in **Table 1**. It should be noted that the maximum heat transfer enhancement $HTE = ((\text{maximum Nusselt number}) Nu_{max} / Nu_0$ (without wavy wall)) takes place for case (2) and at wave amplitude $A=-0.5$, so this case represents the optimum between the studied cases for best heat transfer rate.

CONCLUSIONS

The finite volume method with collocated grid is used to analyze the flow field and heat transfer in wavy channel with discrete heating. The results show that the maximum heat transfer enhancement in the studied cases is in the case where the wavy wall placed on the upper wall over the sources and half wave over each source.

REFERENCES

[1]Goldstein, L., and Sparrow, Jr. E. M., "Heat/Mass Transfer Characteristics for flow in a corrugated wall channel" *Journal of Heat Transfer*, Vol. 99, 1977.

[2]Wang C.C., Chen C.K., "Forced convection in a wavy-wall channel, *Int. J. of Heat Mass Transfer* Vol.45 , pp. 2587–2595, 2002.

[3]Haitham M., Bahaidarah S. and Anand, N. K. "Numerical study of heat and momentum transfer in channels with wavy walls" *Numerical Heat Transfer, Part A*, 47:417–439, 2005.

[4]Esam, M. Alawadhi, and Raed, I. Bourisli, "The role of periodic vortex shedding in heat transfer for transient pastille flow inside wavy channels," *Int. J. of Natural sciences and Engineering*, pp. 179-182, 2009.

[5]Rhie, C. M., and Chow, W. L., "Numerical Study of the Turbulent Flow Past an Airfoil with Trailing Edge Separation", *AIAA Journal*, Vol. 21, pp. 1525-1532, 1983.

[6]Wang Y. and Komori S., On the improvement of the SIMPLE-like method for flows with complex geometry, *Heat and Mass Transfer* 36, 71-78, 2000.

[7]Ferziger, J. H., and Peric, M., "Computational Methods for Fluid Dynamics", Springer-Verlag Berlin Heidelberg, 1996.

Table 1 Maximum Heat Transfer Enhancement (HTE) and corresponding wavy wall amplitude (A) for each source and all cases.

Case	Source	A	HTE=Nu max/Nu ₀
1	1	-0.5	1.7
	2	-0.5	1.5
	3	0.5	1.7
2	1	-0.5	2
	2	-0.5	1.7
	3	-0.5	1.7
3	1	0.5, -0.5	1.8
	2	0.5, -0.5	1.6
	3	0.5, -0.5	1.6
4	1	0.5, -0.5	1.7
	2	0.5, -0.5	1.6
	3	0.5, -0.5	1.6

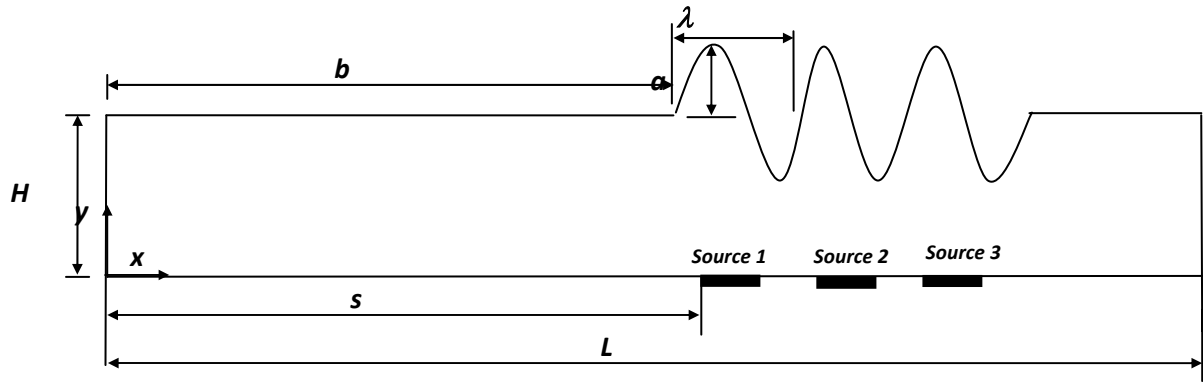


Figure 1 Details of channel geometry and coordinates

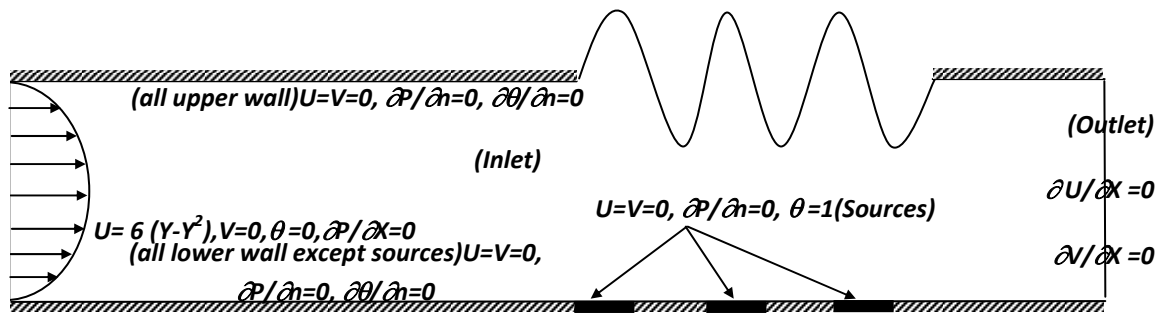


Figure 2 Boundary Conditions.

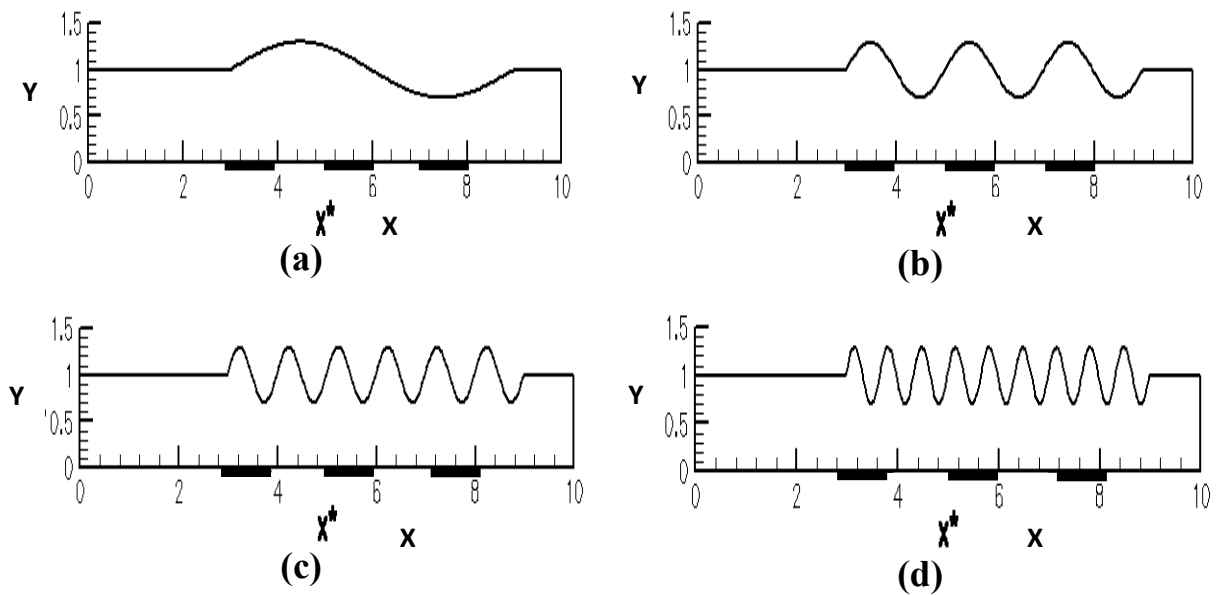


Figure 3 Cases of study, (a): case (1) $w = 1$, (b): case (2) $w = 3$, (c): case (3) $w = 6$, (d): case (4) $w = 9$

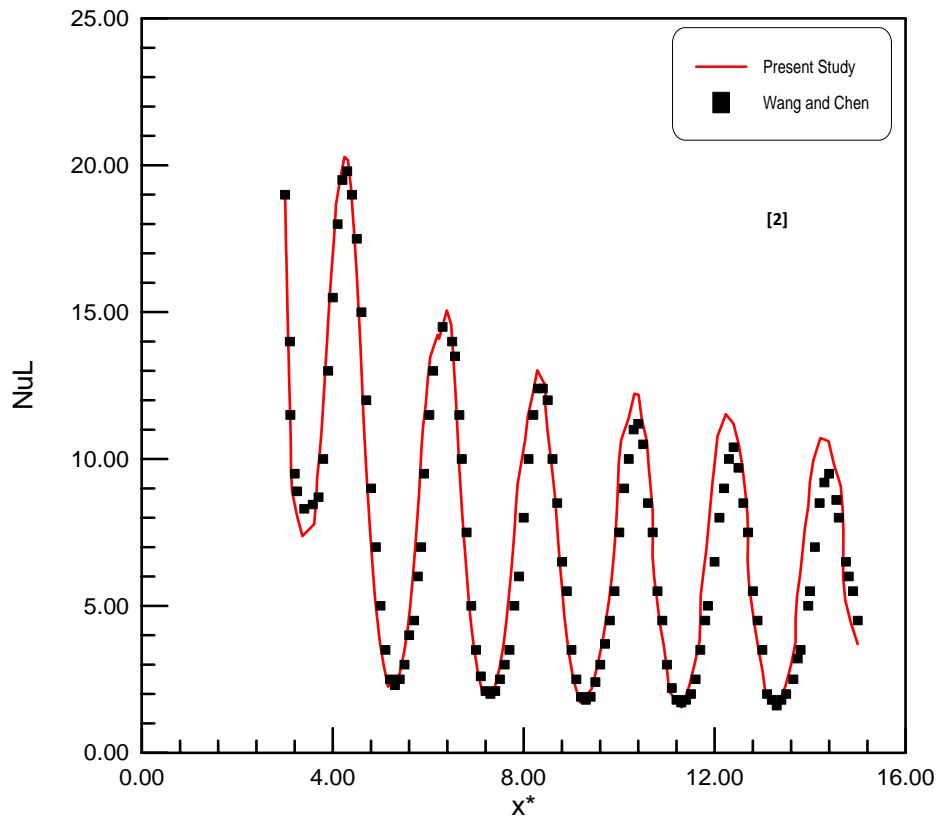


Figure 4 Comparison between the local Nusselt number of present study and that of Wang and Chen (A=0.1), Re=500, Pr = 6.93.

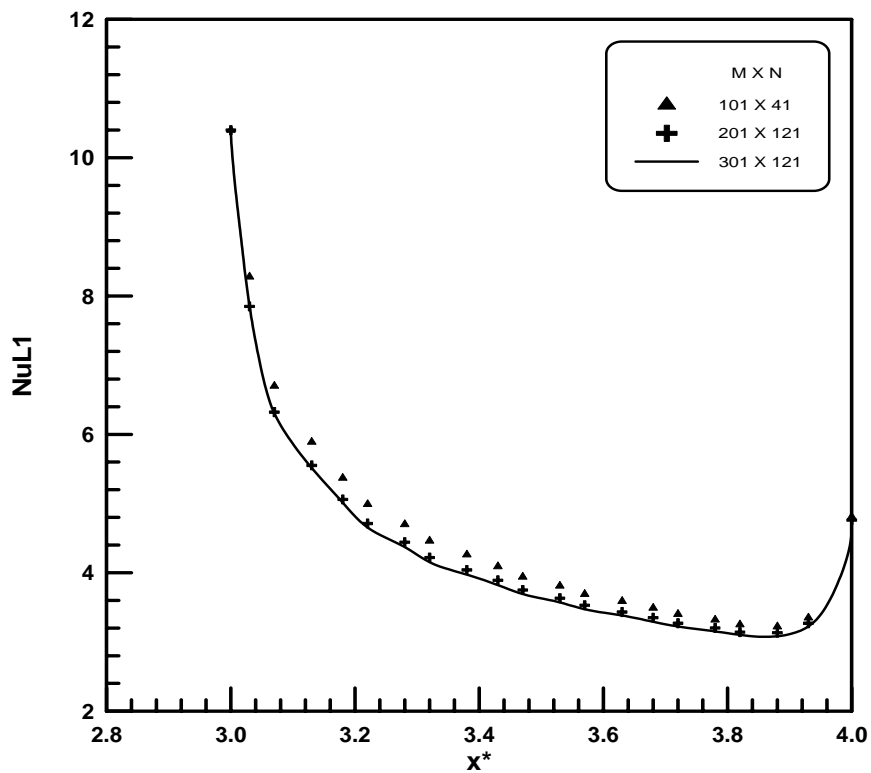


Figure 5 Grid Independence Test (GIT) for source (1) for A=0, Re=50.

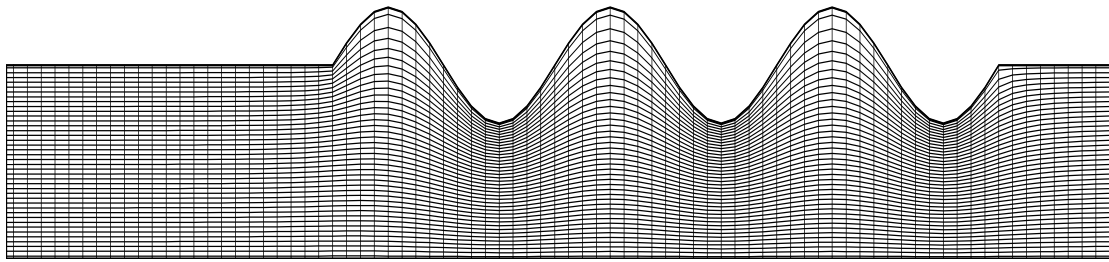


Figure 6 Elliptic Grid System for the channel for (M x N = 81 x 41)

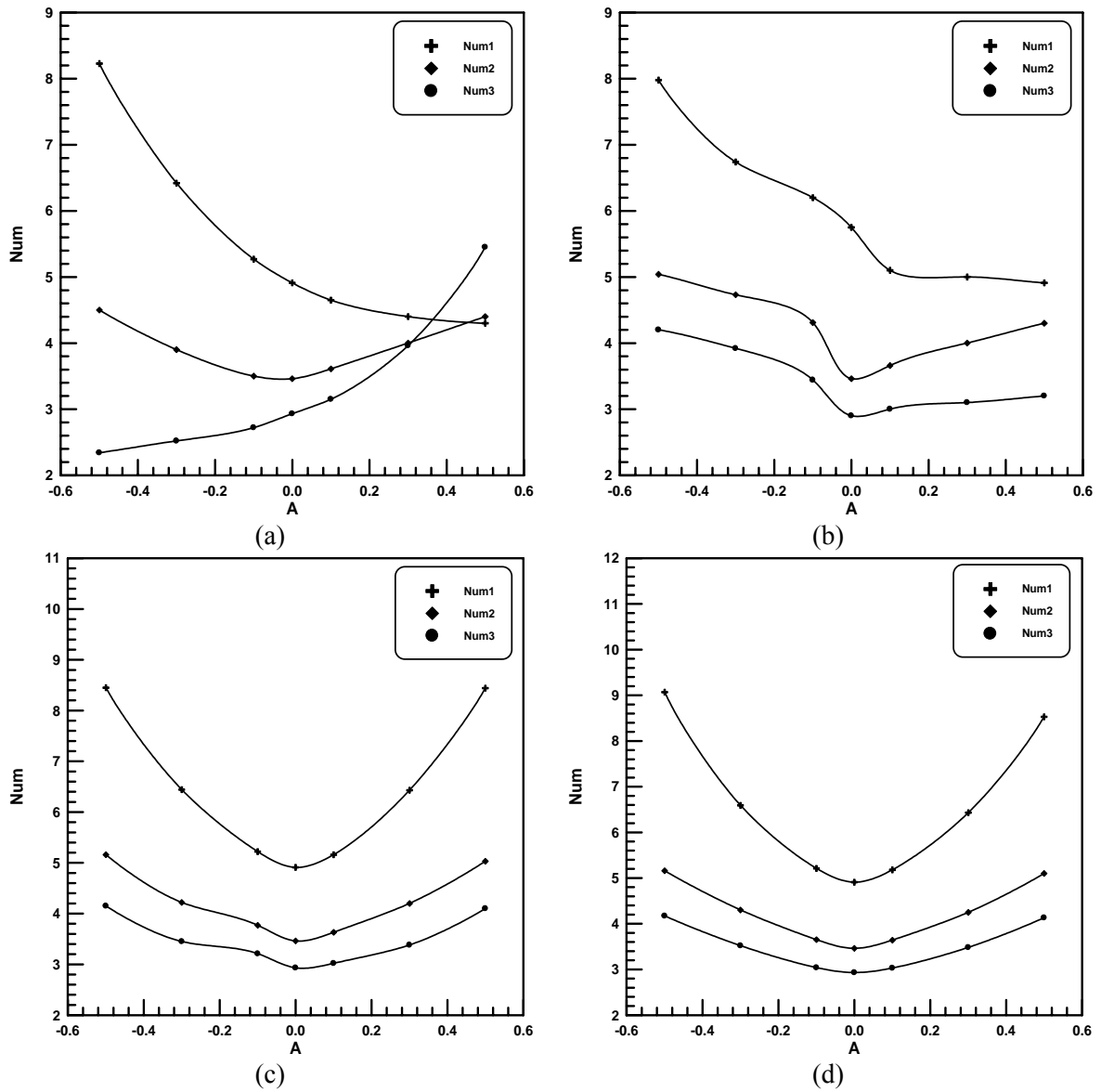


Figure 7 Effect of wave amplitude on the average Nusselt Number for Re=50, (a): Case (1), (b): Case (2), (c): Case (3), (d): Case (4)

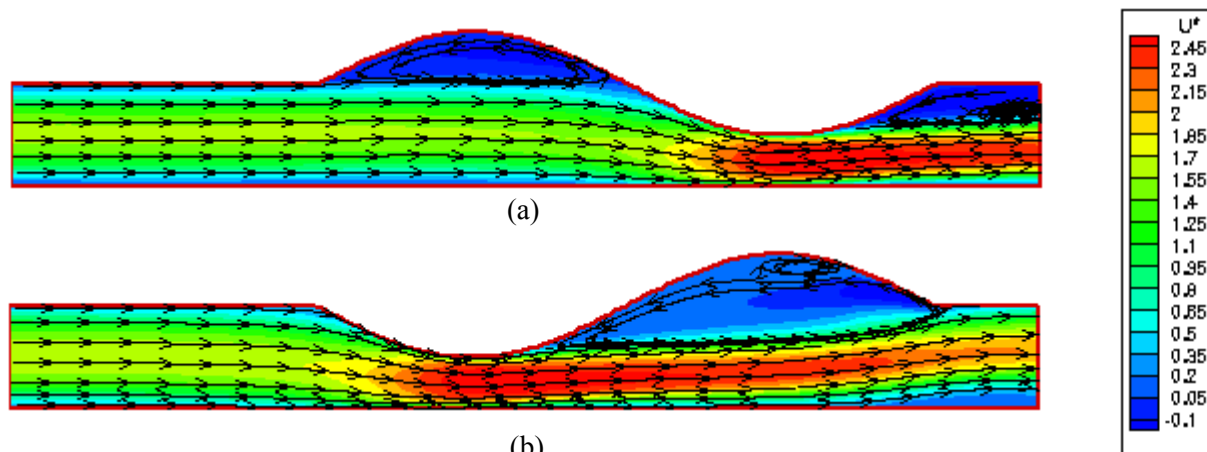


Figure 8 Axial velocity contour and streamline for case (1) and $Re=500$
 (a) $A = 0.5$, (b) $A = -0.5$

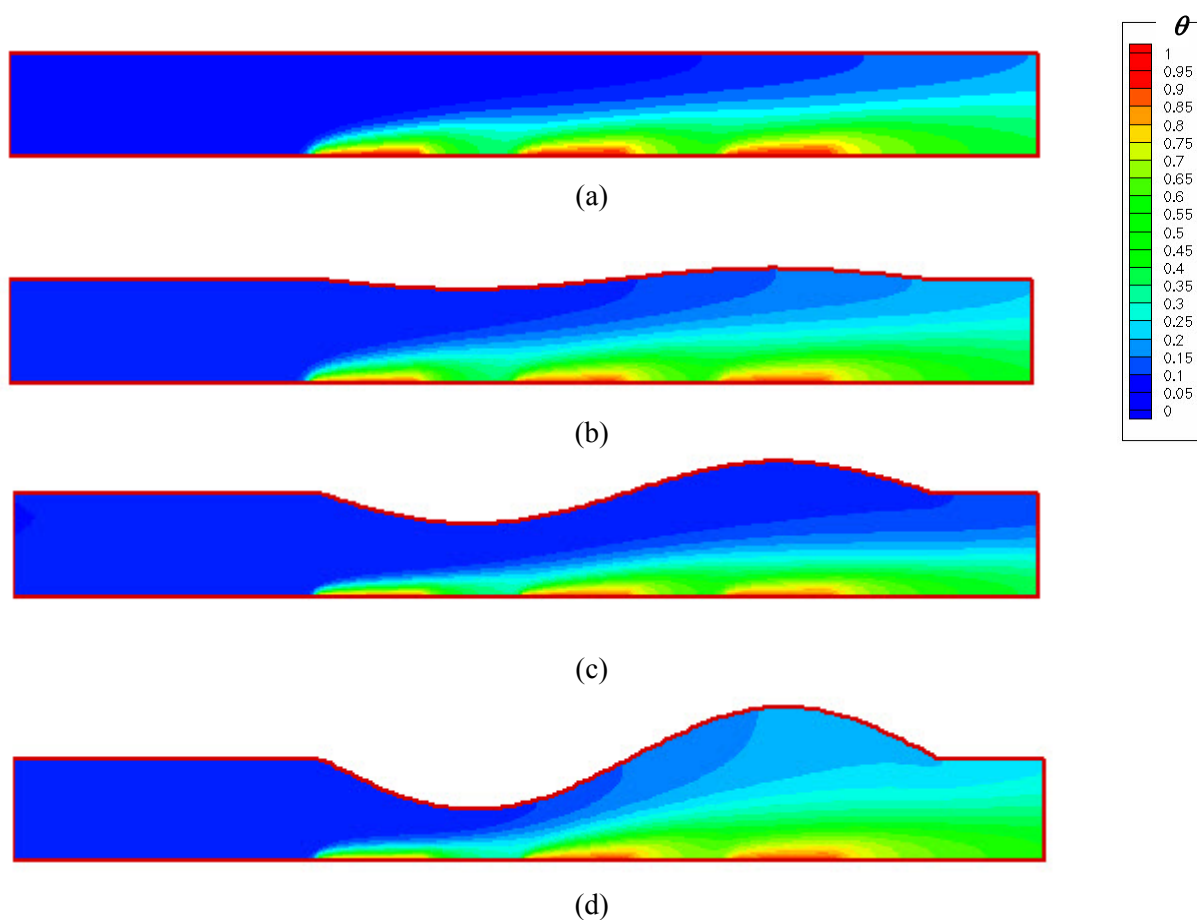


Figure 9 Temperature contour for (Case 1, $w = 1$), $Re = 50$
 (a) $A = 0$, (b) $A = -0.1$, (c) $A = -0.3$, (d) $A = -0.5$

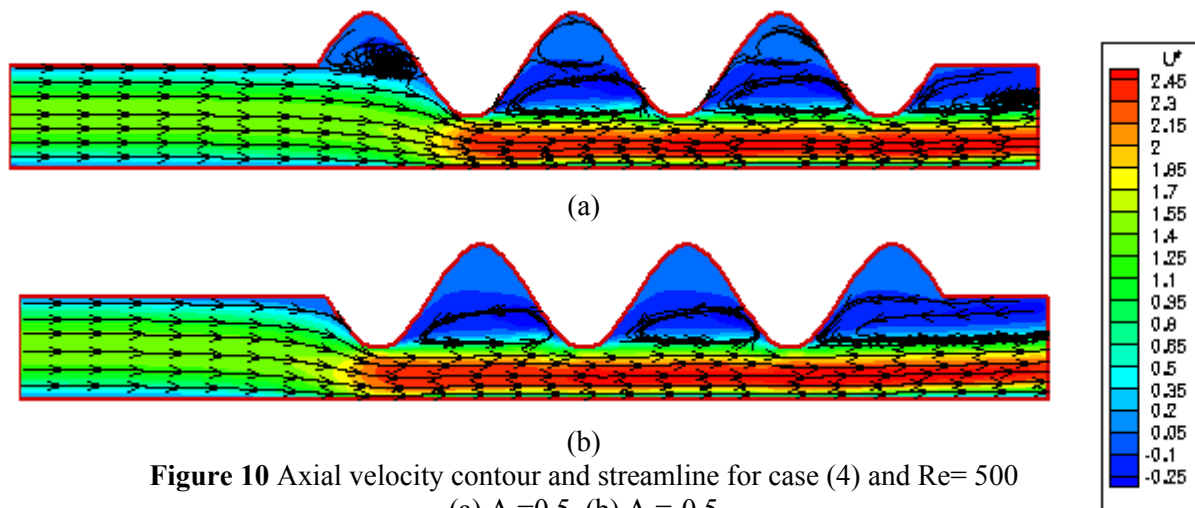


Figure 10 Axial velocity contour and streamline for case (4) and $Re = 500$
 (a) $A = 0.5$, (b) $A = -0.5$

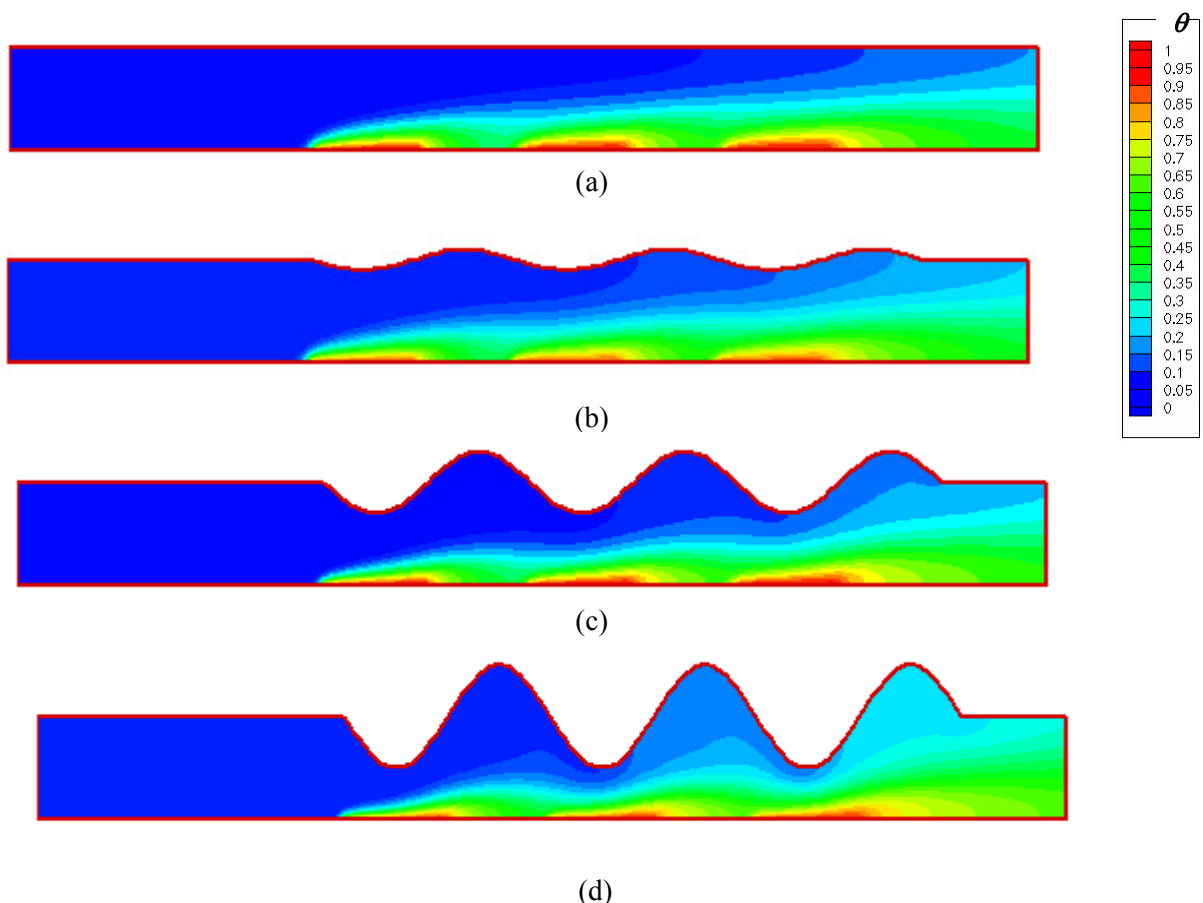


Figure 11 Temperature contour for (Case 1, $w = 1$), $Re = 50$
 (a) $A = 0$, (b) $A = -0.1$, (c) $A = -0.3$, (d) $A = -0.5$